ENVIRONMENTAL RESEARCH
LETTERS

CrossMark

OPEN ACCESS

RECEIVED
27 September 2024

REVISED
11 November 2024

ACCEPTED FOR PUBLICATION
12 December 2024

PUBLISHED
27 December 2024



LETTER

# Toward spatio-temporal models to support national-scale forest carbon monitoring and reporting

Elliot S Shannon[1,2,8,*], Andrew O Finley[1,2,8], Grant M Domke[3], Paul B May[4], Hans-Erik Andersen[5], George C Gaines III[6] and Sudipto Banerjee[7]

[1] Department of Forestry, Michigan State University, East Lansing, MI, United States of America
[2] Department of Statistics and Probability, Michigan State University, East Lansing, MI, United States of America
[3] USDA Forest Service, Northern Research Station, St. Paul, MN, United States of America
[4] Department of Mathematics, South Dakota School of Mines and Technology, Rapid City, SD, United States of America
[5] USDA Forest Service, Pacific Northwest Research Station, Seattle, WA, United States of America
[6] USDA Forest Service, Rocky Mountain Research Station, Missoula, MT, United States of America
[7] Department of Biostatistics, University of California, Los Angeles, Los Angeles, CA, United States of America
[8] These authors contributed equally to this work.
[*] Author to whom any correspondence should be addressed.

**E-mail:** shann125@msu.edu

**Keywords:** spatio-temporal, small area estimation, Bayesian, carbon, NFI

Supplementary material for this article is available online

## Abstract

National forest inventory (NFI) programs provide vital information on forest parameters' status, trend, and change. Most NFI designs and estimation methods are tailored to estimate status over large areas but are not well suited to estimate trend and change, especially over small spatial areas and/or over short time periods (e.g. annual estimates). Fine-scale space-time indexed estimates are critical to a variety of environmental, ecological, and economic monitoring efforts. In the United States, for example, NFI data are used to estimate forest carbon status, trend, and change to support national, state, and local user group needs. Increasingly, these users seek finer spatial and temporal scale estimates to evaluate existing land use policies and management practices, and inform future activities. Here we propose a spatio-temporal Bayesian small area estimation modeling framework that delivers statistically valid estimates with complete uncertainty quantification for status, trend, and change. The framework accommodates a variety of space and time dependency structures, and we detail model configurations for different settings. The proposed framework is used to quantify forest carbon dynamics at an annual county-level across a 14 year period for the contiguous United States. Also, using an analysis of simulated data, we compare the proposed framework with traditional NFI estimators and offer computationally efficient algorithms, software, and data to reproduce results for benchmarking.

## 1. Introduction

Given the ecological and economic importance of forests, national forest inventory (NFI) programs have been implemented to perform large-scale forest monitoring. Data generated by these programs serve as an important resource for quantifying the extent and magnitude of long-term shifts in forest structure and health [1]. For example, signatory countries of the United Nations Framework Convention on Climate Change (UNFCCC) look to their respective NFI programs to inform required annual economy-wide greenhouse gas (GHG) emission and removal reports [2]. Further, a variety of user groups rely on NFI data in their efforts to monitor and mitigate GHG emissions at smaller scales. Traditionally, NFI programs provide design-based estimates for forest parameters based on measurements taken on a forest inventory plot network [3–5]. To achieve desired levels of estimate precision, these methods require repeated costly measurements from a dense network of inventory plots; hence, to improve cost efficiency, we seek methods that can deliver comparable inference using fewer resources. Moreover, NFI programs increasingly seek estimates within smaller spatial, temporal, and biophysical extents than can be reasonably delivered via design-based methods [6–8]. To meet these evolving user needs, estimation methods for inference on small areas—known as small area estimation (SAE)—have recently been applied to NFI data [9–13]. Here, 'small area' refers to any domain of interest that contains too few observations to deliver accurate direct (i.e. design-based) estimates. Most SAE methods aim to improve inference in small areas by leveraging observations from within and outside the domain of interest, auxiliary information correlated with the outcome (or response) variables, and statistical models describing their relationship.

Though inference on small area parameters may proceed from the probabilistic nature of a sample design (e.g. [14–16]), most contemporary SAE methods rely on statistical models for inference [17]. Both design- and model-based methods have been used in the statistical and forestry/ecology literature (see, e.g. [18–22]. The design-based approach assumes a fixed finite population, with population parameters accessible without error if all population units are observed. Randomness is imposed through a randomized sampling design used to select population units into a sample. This mode of inference is effective when there is sufficient data to estimate population parameters of interest and assess variability in those estimates. However, if there is a paucity of data, e.g. due to prohibitive collection costs, then a model-based approach capable of borrowing information from auxiliary data and dependence among population units over space and/or time might be necessary (for model-based as well as fully Bayesian perspectives to inference for finite populations see [23–25]). In applications considered here, we assume the population is a realization from a data-generating stochastic process, and hence we pursue model-based SAE.

SAE methods can generally be classified into two groups: unit-level and area-level models. Unit-level models are constructed at the population unit level, which is the minimal unit that can be sampled from a population. For NFI data, these population units correspond to field plot centers, whose locations may be viewed as occurring over a continuous spatial domain. Unit-level models characterize the relationship between outcome variables measured on sampled population units with auxiliary data available for all population units. Small area prediction proceeds by aggregating unit-level predictions that fall within the areal extent of interest [17]. In contrast, area-level models are constructed at the areal unit level, where areal units are pre-defined non-overlapping areas that tessellate the population's extent. Area-level models characterize the relationship between area-specific direct estimates and auxiliary data. Typically, the direct estimates are generated using design-based estimators [17]. In this way, an area-level model uses available auxiliary information to effectively 'adjust' the area-specific direct estimates.

For NFI data indexed in space and time, unit-level models often provide additional flexibility for model specification and benefit from the well developed theory and methods for point-referenced spatio-temporal data [13, 26–29]. However, if sampling locations are unavailable or data are reported for pre-defined areas, then area-level models are frequently pursued. Given the often proprietary nature of NFI plot locations, our current work focuses on area-level models, specifically the Fay–Herriot (FH) model [30]. This class of models have been widely applied to improve inference in settings where only direct estimates are available across areal units.

FH models can incorporate direct estimates, area-specific auxiliary information, and spatio-temporal dependence among areal units to improve inference, and have recently been applied to forest inventory applications (see, e.g. [31–34]). Working within a hierarchical Bayesian framework, [31] included conditional autoregressive (CAR) spatial random effects in a FH model to improve inference for above-ground forest carbon parameters within small areas. This improvement was also shown in [35], where regression coefficients varied spatially to accommodate nonstationary spatial dependence. FH models have also been applied in operational forestry by coupling field and remotely sensed data to improve stand-level estimates [32]. More recently, [36] developed a Bayesian FH model to estimate forest above-ground biomass density across the contiguous United States (CONUS). Their work identified useful remotely sensed predictor variables and advantages to modeling nonstationary relationships using spatially-varying regression coefficients.

Given NFI data often cover large spatial extents and temporally dynamic forest and land use systems, posited models should accommodate spatio-temporal dependence. This dependence should likely extend beyond space- and time-varying intercepts to accommodate nonstationary relationships between the outcome and predictor variables (as shown in [28, 29, 36, 37]). There is a rich literature on spatio-temporal area-level models, much of which originates from public health research (see, e.g. [38–41]). There are, however, few examples of spatio-temporal FH models. Although spatial dependence was not considered, [42] extended a FH model to accommodate time-series data. More recently, [43] developed a spatio-temporal FH model for income data in Spain, where the model incorporated a space- and time-varying intercept.

We aim to provide useful inference for key forest parameters in small areas that cannot be reliably obtained using design-based methods. To this end, we develop a spatio-temporal Bayesian FH model that delivers statistically valid estimates with complete uncertainty quantification for: (1) annual parameters (e.g. status at a given time); (2) trend (e.g. average change over some time interval); and (3) change (e.g. difference between two points in time). The model and approach to parameter estimation were chosen to accommodate features common in NFI data, including: (1) spatial and temporal dependence across areal units; (2) nonstationary relationships with area-level predictor variables; and (3) missing direct estimates due to the often extremely small spatial and temporal extents.

### 1.1. Applications

To meet GHG reporting obligations, the US relies on the NFI from the US Department of Agriculture (USDA) Forest Service Forest Inventory and Analysis (FIA) program for annual forest carbon status, trend, and change estimates [2]. FIA increasingly seek to improve estimate accuracy and precision at finer spatial and temporal scales to meet evolving user group needs (e.g. voluntary and regulatory carbon markets). However, sparse NFI sampling has limited advances in estimating interannual variability in carbon stocks and stock changes across spatial and temporal scales. Given these challenges, the novelty and importance of estimating temporal components in NFI data for small areas is amplified, and provides further motivation for our proposed work.

We present two applications that make use of NFI data collected and developed by the FIA program. The first considers FIA annual county-level estimates and explores forest carbon status, trend, and change over a 14 year study period across the CONUS. The second uses a simulated population built to mimic NFI data characteristics and used to assess design- and proposed model-based estimators.

## 2. Methods

### 2.1. Direct

Here, we consider spatio-temporal NFI survey data that are collected for a design-based inventory system, where individual inventory plots are repeatedly measured within nonoverlapping discrete areal units and time steps. Specifically, let $y_{i,j,t}$ be the measurement for the $i$th sampling unit in areal unit $j$ at time $t$, where $i = 1, \ldots, n_{j,t}$ indexes sampling units, $j = 1, \ldots, J$ indexes areal units, and $t = 1, \ldots, T$ indexes time steps. Hence, $n_{j,t}$ is the total number of sampling units measured in areal unit $j$ at time $t$. Our goal is to learn about a latent parameter of interest, denoted $\mu_{j,t}$, which is the population mean for areal unit $j$ at time $t$. In the SAE setting, the $n_{j,t}$ are too small to produce estimates with desired levels of accuracy, but design-based direct estimates may still be calculated and used to inform the subsequent model-based estimate for $\mu_{j,t}$. The design-based direct estimate for $\mu_{j,t}$ is calculated as

$$\hat{\mu}_{j,t} = \frac{1}{n_{j,t}} \sum_{i=1}^{n_{j,t}} y_{i,j,t}. \tag{1}$$

where the estimate variance for (1) is

$$\hat{\sigma}^2_{j,t} = \frac{1}{n_{j,t}\left(n_{j,t}-1\right)} \sum_{i=1}^{n_{j,t}} \left(y_{i,j,t} - \hat{\mu}_{j,t}\right)^2. \tag{2}$$

Often, the areal and/or temporal extent is especially small, and few or no plot measurements are available (i.e. $n_{j,t} \in \{0,1\}$), leading to missing direct estimates $\hat{\mu}_{j,t}$ and/or $\hat{\sigma}^2_{j,t}$. Additionally, when plot measurements in areal unit $j$ at time $t$ are identical, $\hat{\sigma}^2_{j,t}$ will be equal to 0. In these cases, we still would like the SAE model to produce an estimate for $\mu_{j,t}$.

### 2.2. Model

We hope to learn about $\mu_{j,t}$ from its direct estimate $\hat{\mu}_{j,t}$, its associated variance statistic $\hat{\sigma}^2_{j,t}$, and from information borrowed from direct estimates for adjacent areas proximate in space and time. Further, we might glean information about $\mu_{j,t}$ from relationships between $\hat{\mu}_{j,t}$ and area-level predictors. Given the large spatial and temporal extents of NFI data, we expect the impact of these predictors to be nonstationary over space and/or time. Since we consider only discrete space and time, we employ autoregressive structures to capture spatial and temporal correlation. Spatial correlations are usually modeled through structures such as CAR or simultaneous autoregressive models [26, 44]. Similarly, temporal correlations are modeled using autoregressive or dynamic structures. Incorporating spatial and/or temporal correlations in these ways could further improve model estimates for $\mu_{j,t}$, especially in cases where direct estimates are imprecise or missing.

The model we propose is an extension to the traditional FH model to accommodate spatio-temporal data of the form described above. For areal unit $j$ at time $t$ the model is

$$\hat{\mu}_{j,t} = \mu_{j,t} + \delta_{j,t}, \tag{3}$$

$$\mu_{j,t} = \beta_0 + \eta_{0,j,t} + \sum_{k=1}^{p} x_{k,j,t}\beta_k + \sum_{k=1}^{q} \tilde{x}_{k,j,t}\eta_{k,j,t} + \epsilon_{j,t}, \tag{4}$$

where $\delta_{j,t}$ and $\epsilon_{j,t}$ are mutually exclusive error terms distributed as mean zero normal ($N$) distributions with $\delta_{j,t} \overset{ind}{\sim} N(0, \sigma^2_{j,t})$ and $\epsilon_{j,t} \overset{iid}{\sim} N(0, \sigma^2_{\epsilon})$. The regression component in (4) comprises a customary fixed effects regression component $\beta_0 + \sum_{k=1}^{p} x_{k,j,t}\beta_k$ and a spatio-temporally varying regression component $\eta_{0,j,t} + \sum_{k=1}^{q} \tilde{x}_{k,j,t}\eta_{k,j,t}$. Each $x_{k,j,t}$, for $k = 1,\ldots,p$, represents a predictor variable referenced for each areal unit $j$ and time $t$ that comprise the fixed effects regression and $\tilde{x}_{k,j,t}$ represents one of $q \leqslant p$ predictor variables included in the spatio-temporally varying component of the model. The restriction $q \leqslant p$ is not essential, but customary in spatio-temporally varying coefficient models since the $\tilde{x}_{k,j,t}$'s are usually a subset of the $x_{k,j,t}$'s. A Bayesian specification will be completed with prior distributions on all parameters, and $\eta_{0,j,t}$ and $\eta_{k,j,t}$'s will each be endowed with a spatial, temporal, or spatio-temporal distribution.

As defined in (1), the design-unbiased estimate for $\mu_{j,t}$, i.e. $\hat{\mu}_{j,t}$, is based on the survey design and is assumed to provide information about the true, but latent, mean. Traditionally in FH model applications, the design-based sampling-error variance $\hat{\sigma}^2_{j,t}$ estimate, defined in (2), is set as the variance of $\delta_{j,t}$ (see, e.g. [17, 45, 46]). This, however, can have undesirable inferential consequences as exposed by substituting the expression for $\mu_{j,t}$ in (4) into (3). The resulting residual variance is $\mathrm{var}(\epsilon_{j,t} + \delta_{j,t}) = \mathrm{var}(\epsilon_{j,t}) + \hat{\sigma}^2_{j,t}$, where the latter term is now a fixed constant. The estimate for this residual variance depends on the least squares estimates for $\beta_0$, $\beta_k$'s, $\eta_{0,j,t}$, and $\eta_{k,j,t}$'s that, in turn, depend upon the predictor variables in (4). There appears to be no theoretical assurance that these predictor variables will indeed provide a residual variance estimate that is greater than the fixed estimate $\hat{\sigma}^2_{j,t}$. It seems, then, possible that the estimate for $\mathrm{var}(\epsilon_{j,t})$ could be forced to be zero (since it cannot be negative) as a purely numerical consequence of fixing a variance component rather than allowing the data to estimate it. Instead, we prefer to incorporate information from the design-based estimate by modeling this variance parameter as an inverse-Gamma (IG) random variable $\sigma^2_{j,t} \sim \mathrm{IG}\left(\frac{n_{j,t}}{2}, \frac{(n_{j,t}-1)\hat{\sigma}^2_{j,t}}{2}\right)$. Modeling $\sigma^2_{j,t}$ in this way also allows us to more clearly obtain potential information from the observed sample size $n_{j,t}$. Specifically, as $n_{j,t}$ increases, the mean of $\sigma^2_{j,t}$ concentrates near $\hat{\sigma}^2_{j,t}$ and its precision increases.

### 2.3. FIA data

The FIA program measures and monitors more than 300 thousand forest inventory plots in the CONUS [3, 4]. Each year, remeasurements are made at approximately 1/5 or 1/7 of all inventory plots in the eastern US and 1/10 of inventory plots in the west, leading to remeasurement intervals (i.e. inventory cycle lengths) ranging from 5 to 10 years. These data are used to generate design-based estimates for important forest parameters, such as forest carbon densities and totals. Carbon content is estimated using measured tree characteristics and national-scale carbon allometric equations based on a comprehensive database of tree species, characteristics, and spatial patterns, for which species-specific carbon fractions are then applied [47]. For this study, individual live tree above-ground carbon estimates are aggregated at the plot-level and then expanded to a per hectare basis to express carbon density (Mg/ha). We let $y_{i,j,t}$ represent the estimated carbon density for FIA plot $i$ in county $j$ and year $t$.

Here, we consider $J = 3108$ counties that comprise the CONUS and $T = 14$ years of plot measurements from 2008 to 2021. A county-level map of FIA plot sample size (i.e. $n_{j,t}$) is shown in figure S1. Only the base intensity plot network, excluding additional intensification plots collected by some states and agencies, is used in our analysis. Of the $N = 43512$ county and time observations, there are 10627 for which direct estimates are missing. This missingness arises from the absence of measured FIA plots (number of occurrences 1860), the absence of sampling error variance due to $n_{j,t} = 1$ (820), or the sampling error variance equaling 0 in areal units with only carbon density measurements of zero (7947). Figure S3 summarizes missingness by county, much of which is concentrated in western and midwestern counties due to lack of forest, survey implementation, and reporting.

Percent tree canopy cover (TCC) data for the CONUS are produced by the USDA Forest Service as part of the National Land Cover Database [48]. The TCC data are derived from multispectral remote sensing data and have been released as annual maps for years 2008–2021 at a 30-by-30 (m) pixel spatial resolution for the CONUS. These data represent fractional pixel-level TCC expressed as a percentage, which we average for each county and year to produce annual county-level mean TCC (%) shown in figure S2. For use in subsequent models, this TCC variable was centered and scaled to have mean zero and variance one, and denoted as $x_{\mathrm{TCC}}$ where the TCC subscript takes the place of subscript $k$.

FIA forest carbon density estimates come with a caveat and limitation. The FIA program defines forest land as land which has at least 10% canopy cover of trees of any size, or had at least 10% canopy cover of trees in the past, based on the presence of stumps, snags, or other evidence, and that will be naturally or artificially regenerated. FIA records zero carbon density for non-forest plots, although they could have up to 10% TCC. Hence, our direct estimate (computed using both forest and non-forest plots) will be negatively biased. Although this bias might be small, difficulty arises when we wish to attribute change in carbon density to change in forest structure and land use—carbon change results from change in forest land area and/or change in carbon density within forest land (e.g. fewer trees). As articulated by

[49, 50], this is a known caveat and limitation when using FIA data for SAE, but also an opportunity for FIA to consider expanding data collection protocols to better support SAE and other model-based estimation efforts.

### 2.4. FIA data analysis

Details about formulating the full model defined in (3) and (4), submodels of (4) considered as candidate models, model implementation and selection, and supplementary results are provided in section S1.

### 2.5. Simulation study overview

The methodology for the simulation study is presented in section S2 and is based on a population generated using fixed and known parameters that mimic qualities of the FIA annual county-level carbon data. The simulation is designed to evaluate estimator performance at the county-level, which is the level of inferential interest (rather than at the unit-level as pursued in other related studies [51]). Direct and model estimates for carbon status, trend, and change are generated from each of a large number of independent samples taken from the simulated population. Estimates are compared with the true simulated population carbon values using measures that assess estimators' bias, accuracy, and precision. Several candidate models are also compared using formal model fit metrics to understand if these metrics can be used for model selection when the true data are not known (which is the case in practice as illustrated in section S1).

## 3. Results

### 3.1. FIA NFI carbon status, trend, and change

SAE model estimates for county-level live standing tree carbon density (Mg/ha), hereafter referred to as carbon, are presented in this section. Results are presented for the 'best' candidate model, which informs estimates by optimally weighting and pooling space- and time-indexed direct estimates and using a spatially adaptive relationship between carbon and remotely sensed percent TCC data. Candidate models, selection criteria, modeling details, and supplementary results are provided in section S1.

Figure 1 shows carbon status estimates (associated uncertainty estimates are given in figure S6). By design, model and direct carbon estimates across counties and years are similar when the direct estimate is informed using a large sample size, i.e. when there is high confidence in the direct estimate (figure S4).

Carbon trend estimates are shown in figure 2(a). Figure 2(b) shows only those county estimates in figure 2(a) that are significantly different from zero. Here, several expected patterns in carbon increase and decrease emerge. As detailed in [52, 53], and similar studies on forest biomass/carbon change in the CONUS, factors including fire, insect, disease, harvest, and changing forest age and land use drive the observed patterns of carbon loss in western counties and portions of the Ohio River basin. In contrast, the increase in carbon in the southeast and Maine is mainly due to increases in industrial forest operations, changes in forest age and structure, and increased forest productivity [53, 54]. Table 1 lists the 10 counties shown in figure 2(b) with the greatest carbon trend increase and decrease.

In addition to carbon density trends, it is instructive to quantify carbon total trends that are obtained by scaling carbon density by county area (ha), shown in figures 2(c) and (d). Table S2 lists the 10 counties shown in figure 2(d) with the greatest carbon total trend increase and decrease. Given the large area of western counties and negative carbon density trend, the 10 counties with the greatest total carbon losses are in California, Oregon, Washington, and Idaho. The large land area counties in Maine and positive carbon density trend, results in Maine counties dominating the total carbon gains.

Figure 3 shows direct and model carbon estimates for the two counties with the greatest negative and positive estimates in figure 2(b). As recorded in table 1, Lake, California has the most negative estimate. Over the study period, Lake County's estimate was −1.25 (−1.62, −0.88) (Mg/ha/yr). This negative trend is evident in Lake County's annual model estimates shown in figure 3(a). Much of Lake County's carbon loss occurred in 2018 as a result of the River, Ranch, and Pawnee Fires that burned an estimated 48 400 (ha) [55, 56]. The effect of these 2018 fires is clearly seen in the model estimates and TCC values in figure 3(a). Given the relatively small sample sizes, it is not surprising that direct estimates do not capture the impact of fire on forest carbon. With lack of direct estimate information, the model learns from TCC, which clearly shows a loss of canopy cover starting in 2018. In contrast, Escambia, Alabama has the most positive estimate. Over the study period, Escambia County's estimate was 0.92 (0.67, 1.20) (Mg/ha/yr). This positive trend is seen in figure 3(b) and reflects carbon accumulation in the county's intensively managed softwood plantations. With few exceptions, the model yields improved uncertainty quantification compared with the direct estimates—as seen when comparing 95% interval bar widths in figure 3 and comparable figures for all other counties provided in section S1.7.

For administrative and some reporting purposes, FIA partitions the CONUS into four regions shown in figure S8: Northern; Pacific Northwest; Rocky Mountain; Southern. Carbon trend and change estimates by FIA region are given in table 2 and

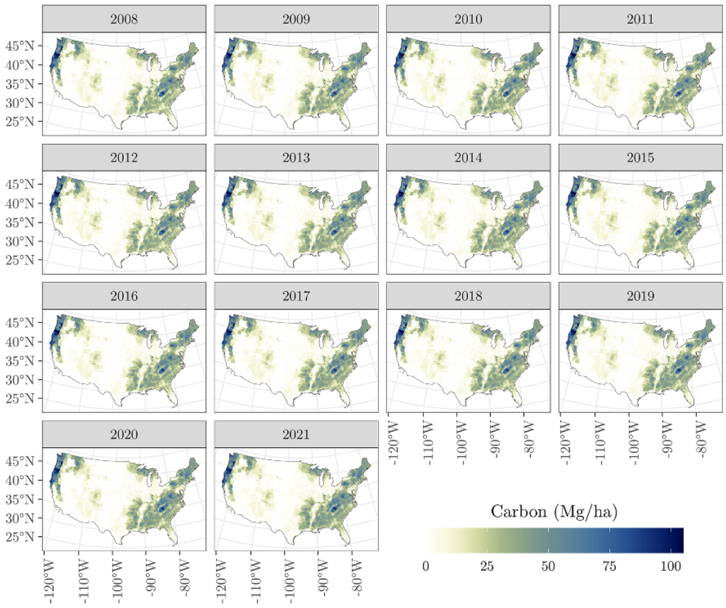


**Figure 1.** Model estimated mean carbon by county and year.

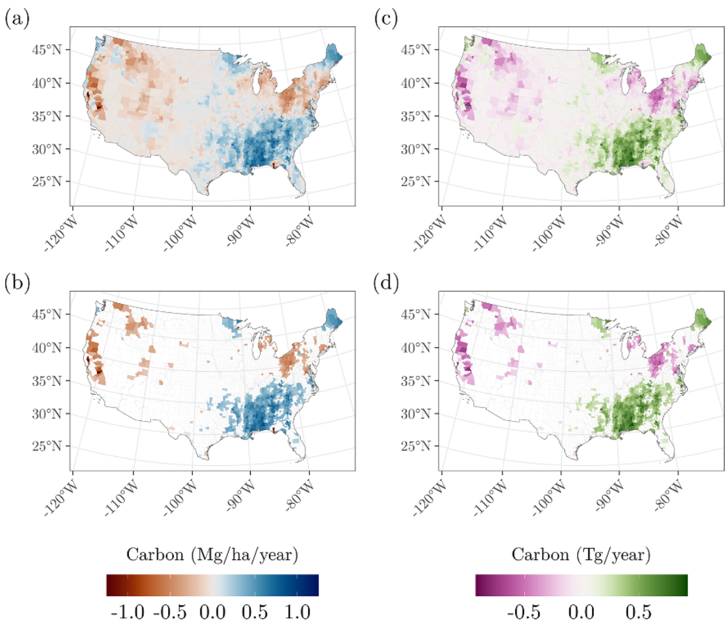


**Figure 2.** (a) Model estimated carbon trend (Mg/ha/yr). (b) Counties from (a) that have 95% credible intervals that exclude zero. (c) Model estimated carbon trend (Tg/yr). (d) Counties from (c) that have 95% credible intervals that exclude zero.

capture regional patterns seen in figure 2 and regional aggregate estimates given in figure S9. Specifically, over the 14 year period, we see no significant change in carbon in the Northern region, significant carbon loss in the Pacific Northwest and Rocky Mountain regions, and significant carbon gain in the Southern region.

### 3.2. Simulation study

Results for the simulation study are presented in section S3. Simulation study results show that: 1) all estimators are biased when the sample size is small (figure S13(a)); 2) models yield improved accuracy and uncertainty quantification over the direct estimator (figure S13(b)); 3) models weight direct

**Table 1.** Ten counties with the greatest decrease and increase in model estimated carbon trend (Mg/ha/yr) from figure 2(b). Estimates are medians with 95% credible interval values given in parentheses.

| Decreasing | | | Increasing | | |
|---|---|---|---|---|---|
| State | County | Carbon | State | County | Carbon |
| California | Lake | −1.25 (−1.62, −0.88) | Alabama | Escambia | 0.92 (0.67, 1.20) |
| Florida | Calhoun | −1.21 (−1.63, −0.76) | Georgia | Cobb | 0.87 (0.58, 1.17) |
| California | Mariposa | −1.19 (−1.57, −0.77) | Tennessee | Rhea | 0.86 (0.59, 1.15) |
| Florida | Gulf | −0.94 (−1.40, −0.52) | Mississippi | Hancock | 0.85 (0.55, 1.14) |
| California | Tuolumne | −0.76 (−1.04, −0.48) | Alabama | Dallas | 0.83 (0.58, 1.07) |
| California | Shasta | −0.71 (−0.98, −0.44) | Mississippi | Harrison | 0.82 (0.52, 1.10) |
| Pennsylvania | Allegheny | −0.67 (−0.92, −0.42) | Alabama | Conecuh | 0.82 (0.54, 1.10) |
| California | Napa | −0.66 (−1.00, −0.34) | Alabama | Greene | 0.81 (0.54, 1.07) |
| Virginia | Falls Church | −0.64 (−1.11, −0.21) | Mississippi | Stone | 0.81 (0.55, 1.08) |
| Ohio | Carroll | −0.63 (−0.93, −0.34) | Georgia | Polk | 0.80 (0.55, 1.07) |

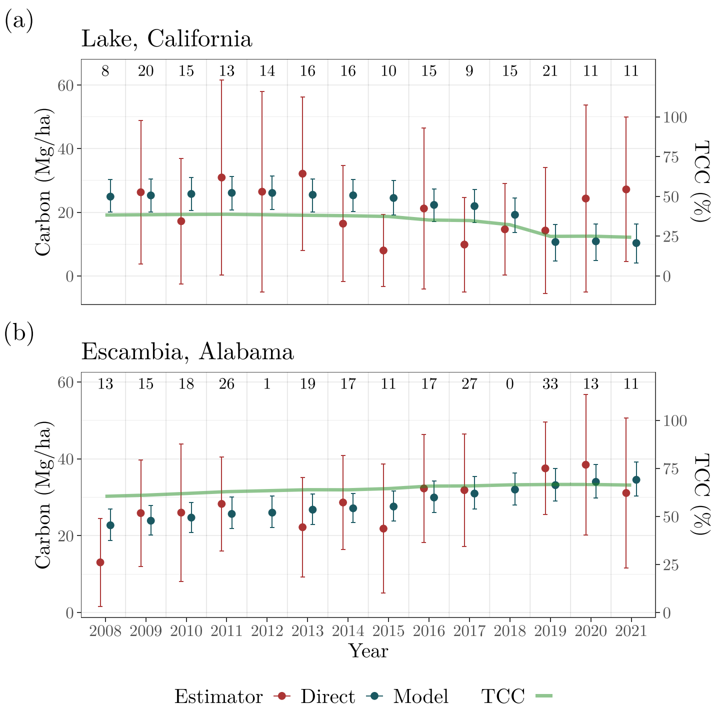


**Figure 3.** Direct and model carbon estimates along with TCC values for counties with the greatest negative and positive values given in table 1. County and year sample size used for the direct is given across the top of each subpanel. Estimate means and medians are shown as points with 95% confidence and credible interval bars for direct and model estimates, respectively. When sample size is ⩽2 or all observations are zero, the direct estimate is not available, e.g. Escambia, Alabama in 2012 and Lake, California in 2008, respectively.

**Table 2.** Left column, model estimated carbon trend by FIA region from 2008 to 2021. Right column, model estimated total carbon change by FIA region between 2008 and 2021. Estimates are medians with 95% credible interval values given in parentheses.

| FIA Region | Trend (Tg/yr) | Change (Tg) |
|---|---|---|
| Northern | −1.94 (−6.74, 3.42) | 43.03 (−43.05, 137.98) |
| Pacific Northwest | −9.55 (−14.71, −5.34) | −101.01 (−186.91, −23.12) |
| Rocky Mountain | −12.86 (−19.46, −6.13) | −137.03 (−285.29, −1.29) |
| Southern | 44.32 (36.83, 50.55) | 660.45 (534.73, 781.08) |

estimates according to sample size (figure S14); 4) popular fit metrics are useful for selecting models of appropriate complexity (table S3). For estimates of trends and change, the models are able to deliver improved accuracy and precision with bias comparable to the direct estimator and coverage rate closer to the expected 95% (figures S15 and S16, respectively).

## 4. Discussion and summary

The FIA data analysis and simulation study demonstrate the proposed model's utility for delivering small area estimates to support estimation and reporting across spatial and temporal scales. The SAE model is assembled using components that are well documented in the statistical literature. In the current setting, the FH model provides a mechanism to learn from direct estimates, predictor variables, and spatially and temporally structured random effects. Casting this model into a Bayesian estimation framework provides additional opportunities to glean information from the data and survey design. For example, our proposed informative IG prior on $\sigma^2_{j,t}$ is an intuitive way to obtain potential information from the observed sample size $n_{j,t}$. The Bayesian framework also provides easy access to posterior distributions derived from the latent mean, e.g. total, trend, and change, for both individual areal units and aggregates of areal units. Further, inference from areal units with no observations is available via the latent mean's posterior predictive distribution, which allows us to make spatially and temporally complete estimates (e.g. for every county and year in the CONUS). This ability to use auxiliary information to adjust/inform direct estimates seems particularly useful for meeting evolving inferential demands placed on existing NFI programs.

Although the proposed model demonstrates distinct advantages to traditional methods, several limitations still persist. SAE models, including the one highlighted here, simply adjust or smooth the direct estimate. If there are issues with the direct estimate, then those issues persist in the model estimate. For example, the simulation study showed that counties with small sample sizes had biased direct estimates and those biases might persist in the model estimates. However, if the adjacent areal units and/or times had more reliable data or larger sample sizes, then the structured random effects shrink the mean toward the average of the proximate neighbors, which could mitigate bias. In fact, one reason why CAR random effects are popular in SAE is because of this bias reduction in sparsely populated regions. The simulation study identified clear advantages to using the model, including improved accuracy and uncertainty quantification in most cases.

Adopting the FH model in our current data setting does not come without some drawbacks which require further consideration. First, if all observations within an areal unit have the same value, there is no direct variance estimate and, hence, that information is not available to train the model—it is treated as missing although it provides valuable information. In our study, this occurred when all plots within a county and year had zero carbon and, in such cases, the model relied on the TCC predictor and random effects to inform the posterior predictive distribution. Second, the FH model is most often applied to continuous and Normally distributed variables, although there are transformations that might accommodate discrete count-like variables, see, e.g. [57]. There are many forest variables that do not have Normal support or lend themselves well to transformation, and in such cases the FH model will not be suitable. Lastly, area-level models, as presented here, do not support prediction for units not included in the initial adjacency matrix used to define spatial CAR random effects. If inference for a new areal unit is needed, the unit must be added to the adjacency matrix and the model refit. If any of these limitations are prohibitive and NFI plot measurements are indexed in space and time, then one might consider unit-level models based upon point-referenced geostatistical models.

NFIs provide critical information on the ecological health and economic viability of forests. As generational investments are being made in the US and beyond to mitigate climate change, NFI programs will continue to be tasked with producing finer spatial and temporal resolution estimates of forest parameter status, trend, and change to support initiatives like forest carbon monitoring required by the UNFCCC and the Paris Agreement. Financial circumstances limit most NFI programs' ability to collect sufficient data to meet these user needs, especially when estimates are provided by traditional design-based methods. SAE models, like those proposed here, can bridge this gap and allow NFIs to continue providing high-quality and reliable estimates and associated uncertainties for key forest parameters to evaluate existing land use polices and practices, and inform future decision making.

## Data availability statement

The data that support the findings of this study are openly available at the following URL/DOI: https://datadryad.org/stash/share/cVfMuUvUEmIbNy1xDtjTP6VwsJoBWF6SMZuao5nX1w4.

## Acknowledgments

This work was supported by the USDA Forest Service, NSF DEB-2213565, and NASA CMS grants Hayes (CMS 2020). The findings and conclusions in this publication are those of the author(s) and should not be construed to represent any official US Department of Agriculture or US Government determination or policy. Banerjee has been supported, in part, by the National Science Foundation (NSF) from grant NSF/DMS 2113778.

## ORCID iDs

Elliot S Shannon https://orcid.org/0000-0002-0856-878X
Grant M Domke https://orcid.org/0000-0003-0485-0355
Hans-Erik Andersen https://orcid.org/0000-0002-5546-9522
George C Gaines III https://orcid.org/0000-0002-4341-6802
Sudipto Banerjee https://orcid.org/0000-0002-2239-208X

## References

[1] Wurtzebach Z, DeRose R J, Bush R R, Goeking S A, Healey S, Menlove J, Pelz K A, Schultz C, Shaw J D and Witt C 2019 Supporting national forest system planning with forest inventory and analysis data *J. For.* **118** 289–306
[2] Domke G M, Walters B F, Giebink C L, Greenfield E J, Smith J E, Nichols M C, Knott J A, Ogle S M, Coulston J W and Steller J 2023 *Greenhouse gas Emissions and Removals From Forest Land, Woodlands, Urban Trees and Harvested Wood Products in the United States, 1990–2021* (U.S. Department of Agriculture, Forest Service) (https://doi.org/10.2737/WO-RB-101)
[3] Bechtold W A and Patterson P L (eds) 2005 *The Enhanced Forest Inventory and Analysis Program: National Sampling Design and Estimation Procedures* (U.S. Department of Agriculture, Forest Service, Southern Research Station)
[4] Westfall J A, Coulston J W, Moisen G G and Andersen H E (eds) 2022 Sampling and estimation documentation for the enhanced forest inventory and analysis program: 2022 *General Technical Report* NRS-207 (U.S. Department of Agriculture, Forest Service, Northern Research Station)
[5] Tomppo E, Schadauer K, McRoberts R E, Gschwantner T, Gabler K and Ståhl G 2009 *National Forest Inventories: Pathways for Common Reporting* vol 1 (Springer)
[6] Köhl M, Magnussen S and Marchetti M 2006 *Sampling Methods, Remote Sensing and GIS Multiresource Forest Inventory* (Springer)
[7] Breidenbach J and Astrup R 2012 Small area estimation of forest attributes in the Norwegian National Forest Inventory *Eur. J. For. Res.* **131** 1255–67
[8] Prisley S, Bradley J, Clutter M, Friedman S, Kempka D, Rakestraw J and Sonne Hall E 2021 Needs for small area estimation: perspectives from the us private forest sector *Front. For. Glob. Change* **4** 746439
[9] Hou Z, Domke G M, Russell M B, Coulston J W, Nelson M D, Xu Q and McRoberts R E 2021 Updating annual state-and county-level forest inventory estimates with data assimilation and FIA data *For. Ecol. Manage.* **483** 118777
[10] Coulston J W, Green P C, Radtke P J, Prisley S P, Brooks E B, Thomas V A, Wynne R H and Burkhart H E 2021 Enhancing the precision of broad-scale forestland removals estimates with small area estimation techniques *Forestry* **94** 427–41
[11] Schroeder T A, Healey S P, Moisen G G, Frescino T S, Cohen W B, Huang C, Kennedy R E and Yang Z 2014 Improving estimates of forest disturbance by combining observations from Landsat time series with US Forest Service Forest Inventory and Analysis data *Remote Sens. Environ.* **154** 61–73
[12] Lister A J *et al* 2020 Use of remote sensing data to improve the efficiency of national forest inventories: a case study from the United States National Forest Inventory *Forests* **11** 1364
[13] Finley A O, Andersen H E, Babcock C, Cook B D, Morton D C and Banerjee S 2024 Models to support forest inventory and small area estimation using sparsely sampled LiDAR: a case study involving G-LiHT LiDAR in Tanana, Alaska *J. Agric. Biol. Environ. Stat.* **29** 695–722
[14] Breidt F J and Opsomer J D 2017 Model-assisted survey estimation with modern prediction techniques *Stat. Sci.* **32** 190–205
[15] Wojcik O C, Olson S D, Nguyen P H V, McConville K S, Moisen G G and Frescino T S 2022 Gregory: a modified generalized regression estimator approach to estimating forest attributes in the interior Western US *Front. For. Glob. Change* **4** 763414
[16] Affleck D L and Gaines III G C 2023 Model-assisted domain estimation of postfire tree regeneration in the Western US using nearest neighbor techniques *Can. J. For. Res.* **53** 981–95
[17] Rao J N and Molina I 2015 *Small Area Estimation* (Wiley)
[18] Särndal C E, Thomsen I, Hoem J M, Lindley D V, Barndorff-Nielsen O and Dalenius T 1978 Design-based and model-based inference in survey sampling [with discussion and reply] *Scand. J. Stat.* **5** 27–52 (available at: www.jstor.org/stable/4615682)
[19] Särndal C, Swensson B and Wretman J 2003 *Model Assisted Survey Sampling* (*Springer Series in Statistics*) (Springer)
[20] Gregoire T G 1998 Design-based and model-based inference in survey sampling: appreciating the difference *Can. J. For. Res.* **28** 1429–47
[21] McRoberts R E 2010 Probability- and model-based approaches to inference for proportion forest using satellite imagery as ancillary data *Remote Sens. Environ.* **114** 1017–25
[22] Dumelle M, Higham M, Ver Hoef J M, Olsen A R and Madsen L 2022 A comparison of design-based and model-based approaches for finite population spatial sampling and inference *Methods Ecol. Evol.* **13** 2018–29
[23] Little R J 2004 To model or not to model? Competing modes of inference for finite population sampling *J. Am. Stat. Assoc.* **99** 546–56
[24] Ghosh M 2012 Finite population sampling: a model-design synthesis. Statistics in transition new series *Cent. Eur. J. Soc. Sci. Humanit.* **13** 235–42
[25] Banerjee S 2024 Finite population survey sampling: an unapologetic Bayesian perspective *Sankhya* A **86** 95–124
[26] Banerjee S, Carlin B and Gelfand A 2004 *Hierarchical Modeling and Analysis of Spatial Data* (*Chapman & Hall/CRC Monographs on Statistical and Applied Probability* vol 101) (https://doi.org/10.1201/9780203487808)
[27] Cressie N and Wikle C 2011 *Statistics for Spatio-Temporal Data* (*Coursesmart Series*) (Wiley)
[28] Datta A, Banerjee S, Finley A O and Gelfand A E 2016 Hierarchical nearest-neighbor Gaussian process models for large geostatistical datasets *J. Am. Stat. Assoc.* **111** 800–12
[29] May P B and Finley A O 2024 Calibrating satellite maps with field data for improved predictions of forest biomass *Environmetrics* e2892 (arXiv:2407.07134)
[30] Fay R E and Herriot R A 1979 Estimates of income for small places: an application of James-Stein procedures to census data *J. Am. Stat. Assoc.* **74** 269–77
[31] Ver Planck N R, Finley A O, Kershaw J A, Weiskittel A R and Kress M C 2018 Hierarchical Bayesian models for small area estimation of forest variables using LiDAR *Remote Sens. Environ.* **204** 287–95
[32] Temesgen H, Mauro F, Hudak A T, Frank B, Monleon V, Fekety P, Palmer M and Bryant T 2021 Using Fay–Herriot models and variable radius plot data to develop a stand-level inventory and update a prior inventory in the Western Cascades, or, United States *Front. For. Glob. Change* **4** 745916
[33] Cao Q, Dettmann G T, Radtke P J, Coulston J W, Derwin J, Thomas V A, Burkhart H E and Wynne R H 2022 Increased precision in county-level volume estimates in the United States National Forest Inventory with area-level small area estimation *Front. For. Glob. Change* **5** 769917

[34] Stanke H, Finley A O and Domke G M 2022 Simplifying small area estimation with rFIA: a demonstration of tools and techniques *Front. For. Glob. Change* **5** 745874
[35] Chandra H, Salvati N and Chambers R 2015 A spatially nonstationary Fay–Herriot model for small area estimation *J. Surv. Stat. Methodol.* **3** 109–35
[36] May P, McConville K S, Moisen G G, Bruening J and Dubayah R 2023 A spatially varying model for small area estimates of biomass density across the contiguous United States *Remote Sens. Environ.* **286** 113420
[37] Finley A O, Banerjee S and MacFarlane D W 2011 A hierarchical model for quantifying forest variables over large heterogeneous landscapes with uncertain forest areas *J. Am. Stat. Assoc.* **106** 31–48
[38] Waller L A, Carlin B P, Xia H and Gelfand A E 1997 Hierarchical spatio-temporal mapping of disease rates *J. Am. Stat. Assoc.* **92** 607–17
[39] Rushworth A, Lee D and Mitchell R 2014 A spatio-temporal model for estimating the long-term effects of air pollution on respiratory hospital admissions in Greater London *Spat. Spatio-temporal Epidemiol.* **10** 29–38
[40] Rushworth A, Lee D and Sarran C 2017 An adaptive spatiotemporal smoothing model for estimating trends and step changes in disease risk *J. R. Stat. Soc.* C **66** 141–57
[41] Lee D, Rushworth A and Napier G 2018 Spatio-temporal areal unit modeling in R with conditional autoregressive priors using the CARBayesST package *J. Stat. Softw.* **84** 1–39
[42] Rao J N K and Yu M 1994 Small-area estimation by combining time-series and cross-sectional data *Can. J. Stat.* **22** 511–28
[43] Marhuenda Y, Molina I and Morales D 2013 Small area estimation with spatio-temporal Fay–Herriot models *Comput. Stat. Data Anal.* **58** 308–25
[44] Ver Hoef J M, Peterson E E, Hooten M B, Hanks E M and Fortin M J 2018 Spatial autoregressive models for statistical inference from ecological data *Ecol. Monogr.* **88** 36–59
[45] Wang J C, Holan S H, Nandram B, Barboza W, Toto C and Anderson E 2012 A Bayesian approach to estimating agricultural yield based on multiple repeated surveys *J. Agric. Biol. Environ. Stat.* **17** 84–106
[46] Porter A T, Holan S H, Wikle C K and Cressie N 2014 Spatial Fay–Herriot models for small area estimation with functional covariates *Spat. Stat.* **10** 27–42
[47] Westfall J A *et al* 2023 A national-scale tree volume, biomass, and carbon modeling system for the United States *General Technical Report* WO-104 (U.S. Department of Agriculture, Forest Service) (http://dx.doi.org/10.2737/WO-GTR-104)
[48] Housman I, Schleeweis K, Heyer J, Ruefenacht B, Bender S, Megown K, Goetz W and Bogle S 2023 National land cover database tree canopy cover methods v2021.4. *General Technical Report* GTAC-10268-RPT1 (U.S. Department of Agriculture, Forest Service, Geospatial Technology and Applications Center)
[49] Wiener S S, Bush R, Nathanson A, Pelz K, Palmer M, Alexander M L, Anderson D, Treasure E, Baggs J and Sheffield R 2021 United States forest service use of forest inventory data: examples and needs for small area estimation *Front. For. Glob. Change* **4** 763487
[50] Knott J A, Liknes G C, Giebink C L, Oh S, Domke G M, McRoberts R E, Quirino V F and Walters B F 2023 Effects of outliers on remote sensing-assisted forest biomass estimation: a case study from the United States National Forest Inventory *Methods Ecol. Evol.* **14** 1587–602
[51] Emick E, Babcock C, White G W, Hudak A T, Domke G M and Finley A O 2023 An approach to estimating forest biomass while quantifying estimate uncertainty and correcting bias in machine learning maps *Remote Sens. Environ.* **295** 113678
[52] Harris N L *et al* 2016 Attribution of net carbon change by disturbance type across forest lands of the conterminous United States *Carbon Balance Manage.* **11** 24
[53] Hoover C M and Smith J E 2021 Current aboveground live tree carbon stocks and annual net change in forests of conterminous United States *Carbon Balance Manage.* **16** 17
[54] Hogan J A, Domke G M, Zhu K, Johnson D J and Lichstein J W 2024 Climate change determines the sign of productivity trends in US forests *Proc. Natl Acad. Sci.* **121** e2311132121
[55] Tyukavina A *et al* 2022 Global trends of forest loss due to fire from 2001 to 2019 *Front. Remote Sens.* **3** 825190
[56] Shao E 2024 Half their land burned in a decade: the California counties constantly on fire (New York Times) (available at: www.nytimes.com/interactive/2024/08/15/us/california-fires.html)
[57] Ghosh M, Ghosh T and Hirose M Y 2022 Poisson counts, square root transformation and small area estimation *Sankhya* B **84** 449–71